

Scaling of sound emission energy and fracture behavior of cellular solid foods

Marcel B. J. Meinders^{1,2} and Ton van Vliet^{1,2}

¹Wageningen Centre for Food Sciences, P. O. Box 557, 6700 AN Wageningen, The Netherlands

²Wageningen University and Research Centre, P. O. Box 17, 3700 AA Wageningen, The Netherlands

(Received 23 August 2007; revised manuscript received 21 December 2007; published 17 March 2008; corrected 2 April 2008)

A detailed study was performed of the fracture behavior of toasted rusk rolls, a cellular solid food, at different water activities and morphologies. We find that the energies of the emitted sound pulses follow Gutenberg-Richter power laws with characteristic exponents $b \sim 1.5$. The scaling exponents varied only within a range of 0.2 when the method of fracture, humidity, or morphology was changed. However, differences in b were observed, indicating nonuniversal behavior, that seems to be related to morphology and water activity. Also, power law scaling behavior was observed for the waiting time distributions with an exponent $a \sim 1.9$.

DOI: [10.1103/PhysRevE.77.036116](https://doi.org/10.1103/PhysRevE.77.036116)

PACS number(s): 62.20.M-, 05.65.+b, 89.75.Da

I. INTRODUCTION

The mechanical and fracture behavior of solids is an important research field, not only because of the interesting and challenging scientific questions that are involved but also due to the applications it finds in various areas, ranging from studies on earthquakes to building construction and even food perception. Many studies have been published about crack formation and its stability as well as on the sound emitted at high crack speeds [1–6]. Much insight has been gained but a clear understanding of even single-fracture phenomena is still lacking. Fracture behavior can also be treated from a statistical point of view. Inhomogeneous materials may respond to an external load with (micro)fracture events of various magnitudes, producing so-called crackling noise [7]. The statistical distribution of the magnitudes follows, over a broad magnitude range, a power law $N(E) \propto E^{-b}$ with N the number of events, E their size, and b a constant. One of the first reported and most striking examples is that of Gutenberg and Richter who showed this power law scaling for earthquakes. The characteristic exponent b turned out to be about 1.5 and independent of the area and details of the earth system. This universality combined with the scale invariance imply that the fracture behavior of the system is independent of its (microscopic) details. Simple models could therefore be suitable to describe it. This was indicated by Bak *et al.* who introduced the concept of self-organized criticality and explained the power law behavior with $b \sim 1.5$ using a simple avalanche sand-pile model [8,9].

Different kinds of systems have been studied and shown to exhibit crackling phenomena and power law behavior. The characteristic exponents are all in the same range but vary somewhat between materials. For example, for creep experiments on cellular glass $b = 1.5 \pm 0.1$ [10], for crumpling paper $b = 1.3 - 1.6$ [11], for synthetic plaster $b = 1.3 \pm 0.1$ [12], for paper $b = 1.3 \pm 0.1$ [13,14], for fiberglass $b = 2.0 \pm 0.1$ [15,16], for Plexiglas $b = 1.7 \pm 0.1$ [17], and for wood $b = 1.51 \pm 0.05$ [15,16] were found. Recently also differences in b were found for fracture of different types of rocks, where b varied between 1.3 and 1.9 [18]. The underlying reason for these differences in characteristic exponents and how they depend on the microscopic details of the systems is far from understood.

Here we report a detailed study of the fracture behavior of a cellular solid food that may give valuable knowledge about these aspects. We measured the acoustic emission of single-fracture events of toasted rusk rolls under a compressive load. These food products are spongelike structures with cell walls primarily made out of proteins and/or carbohydrates. Because water acts as a plasticizer for these polymers, the mechanical and fracture properties depend strongly on the amount of water present in these products. At low water activity A_w , the material fractures easily in a brittle way producing a lot of noise. At high A_w , the material responds more viscoelastically to an external load, producing less or no sound on fracture [19]. This fracture behavior is strongly related to crispness, which is the most important factor for consumers to judge the quality of these cellular solid food products [20,21].

II. MATERIALS AND METHODS

Fracture experiments were performed on two types of toasted rusk rolls, a commercial one of the Dutch brand Bolletje (Almelo, the Netherlands) and one having a coarser cell structure that was made by TNO (Zeist, the Netherlands) according to a formulation given by Bolletje. A detailed description of the formulation and preparation is given elsewhere [22]. Samples were equilibrated in climate-controlled chambers at standard temperature of 20 °C and relative humidities (RHs) ranging from 30% to 80%.

Samples were fractured in a controlled way by using a Texture Analyzer (Stable Micro Systems, Surrey, U.K.). Stress, strain, and emitted sound were measured simultaneously as a function of time. Different probes to fracture the sample were used: a scalpel (thickness 0.3 mm with a wedge-shaped cutting end 0.75 mm high), a cylinder (diameter 40 mm), and a needle (diameter 0.5 mm). For the fracture experiment with the scalpel, the sample was half of a cylinder (diameter of 70 mm and thickness of 10 mm) which was put on its flat side. For the fracture experiments with the cylinder, a cylindrical sample was used having a thickness of 10 mm and a diameter equal to that of the probe. The fracture experiments with the needle were performed on tetragonal samples with a size of about $70 \times 70 \times 10$ mm³ that were put on their sides. A deformation speed of 0.4 mm/s

was used unless explicitly stated otherwise. Fracture experiments were also performed on a whole rusk roll that was put on its side and crushed between two plates covered with foam. The foam was used to distribute the force across the sample and to prevent fracture of small parts of the rusk roll. For these fracture experiments we used a deformation speed of 0.2 mm/s. The deformation speeds were the best compromises between signal to noise ratio and ability to distinguish individual events. The emitted sound was measured with a calibrated microphone (Brüel & Kjær, Nærum, Denmark) positioned 70 mm from the sample. Both sound and force data were digitized using a portable pulse analog-to-digital converter (Brüel & Kjær, Nærum, Denmark) at a sampling rate of 2^{16} Hz, giving sound pressure in pascals and force in newtons, respectively. All measurements were performed in an acoustically isolated and anechoic chamber reducing outside noise by 50 dB and giving approximately free field sound conditions.

Software was developed using MATLAB (MathWorks) to detect individual events in the acoustic emission and force data and to determine their characteristics. The probe of the texture analyzer is driven by a step motor that produces random noise as well as coherent noise at various specific frequencies up to about 5000 Hz. For the analyses of the acoustic emission data, this noise was reduced by about a factor of 50 (17 dB) by application of a high-pass cutoff filter with a cutoff frequency of 5000 Hz. Because of the short duration of the sound events (about 1 ms) and because most energy is at high frequencies, a cutoff frequency of 5000 Hz turned out to be the best compromise between maximum noise reduction and minimum loss of information.

After filtering, the sound intensity, in W/m^2 , is calculated according to $I = p^2 / (2\rho_a v_a)$ with p the filtered sound pressure, ρ_a the density of air, and v_a the sound velocity in air. Single sound events were determined from the sound intensity data by identifying a set of peaks with intensity larger than a threshold value. The latter was around 10^{-7} W/m^2 and determined from the noise at the beginning of the sound intensity data before the first sound event. The start time of the single sound event is taken to be the time t_0 corresponding to the first sound peak with intensity larger than the threshold. The end time t_e of the event was taken as the time corresponding to the first sound peak that has intensity larger than 1.5 times that of an envelope $I_e = \frac{I_m}{[(t-t_m)/t_{1/2}]^2 + 1}$. Here I_m is the maximum intensity of a single sound event at time t_m that is identified within the region $t_0 < t < t_0 + 2t_{1/2}$, with $t_{1/2} = 0.5$ ms the half-width of the sound event. The start of a new event was identified as the first sound peak with intensity larger than four times the envelope for $t_m < t < t_e$, or as the first sound peak with intensity larger than the threshold value for $t > t_e$. The envelope, criteria, and half-width were chosen after careful analyses of many single sound events. The total sound event energy is calculated as $E = \int_{t_0}^{t_e} I dt$ (in J/m^2). Examples of filtered sound pressure p and single sound events are shown in Sec. III.

Single force events are modeled as a linear increase in force, due to an elastic response of the sample to a deformation, and a sudden drop in force, due to the fracture of a part of the sample. The force drops and start of force rises were

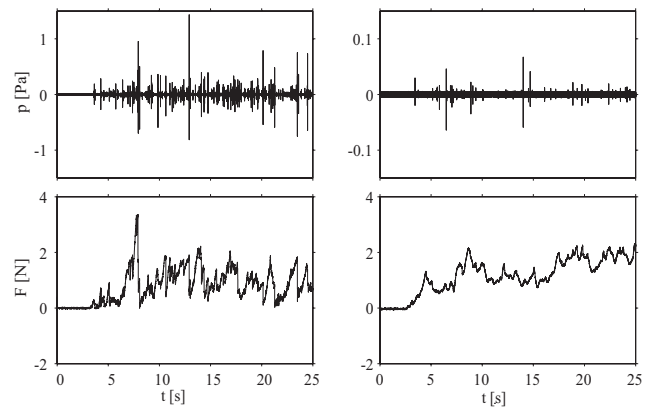


FIG. 1. Sound amplitudes (upper) and applied force (lower) during fracture of toasted rusk roll [fine structure, RH=30% (left) and 70% (right)].

identified as peaks in the derivative of the force data which were filtered using a low-pass filter with a cutoff frequency of 50 Hz. The start and end of the force drop were identified as the maximum and minimum values in the force data which were filtered using a low-pass filter with a cutoff frequency of 150 Hz, nearest to the force drop. Examples of force events are shown below.

III. RESULTS AND DISCUSSION

Figure 1 shows two typical examples of filtered acoustic emission (sound pressure p) and force F data versus time t of a commercial toasted rusk roll, equilibrated at RH of 30% (left panels) and 70% (right panels). The rusk rolls were fractured using the scalpel. Figure 2 shows an enlarged part of Fig. 1. Clear differences in the acoustical emission and force data can be observed. The fresh sample, equilibrated at RH of 30%, fractures in a brittle way under emission of much noise, while much less sound is produced during fracture of the more humid sample. The peaks in the stress-strain

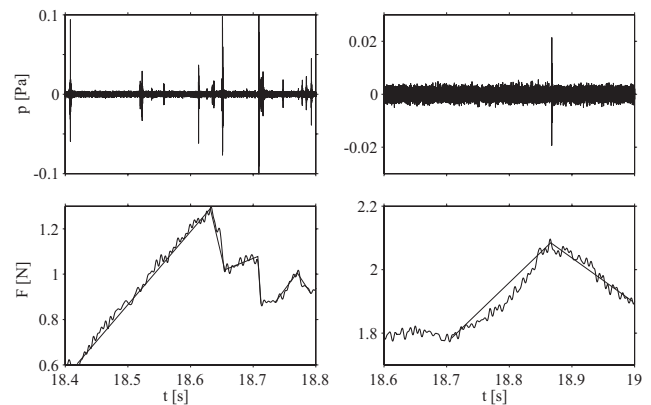


FIG. 2. Blowup of sound amplitudes (upper) and applied force (lower) during fracture of toasted rusk roll [fine structure, RH = 30% (left) and 70% (right)] as shown in Fig. 1. The continuous lines in the applied force graphs (lower) correspond to the force events detected by the software.

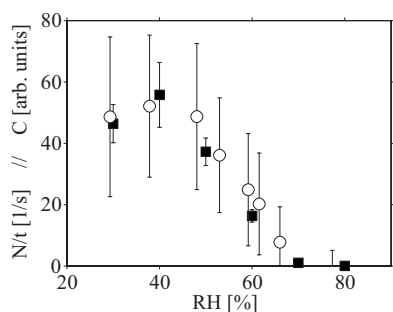


FIG. 3. Averaged number of single sound events per second N/t (■) and crispness C (○) of fine toasted rusk rolls, as scored by a panel (in arbitrary units), as a function of relative humidity RH. Errors are indicated.

curve of the sample equilibrated at RH of 70% are also more rounded than those of the RH=30% sample, indicating more plastic behavior under failure. This is also expressed by the slope of the force drops as detected by our software, which is smaller for the samples equilibrated at large RH than for those equilibrated at small RH. For brittle fracture the slope is determined by the inertia of the force transducer, while at large RH it is determined by the viscoelastic properties of the material. Samples equilibrated at 80% humidity did not produce any sound during failure. Consumers judge the fresh sample as crispy, contrary to the humid one which is judged as being not crispy at all. A clear relation between crispness as sensed by consumers and the characteristics of the fracture data mentioned here is found, as can be seen in Fig. 3 where the averaged number of single sound events per second and crispness of fine toasted rusk rolls, as scored by a panel, is plotted as a function of RH.

Figure 4 shows an example of a single acoustical event detected by our software. Figure 5 shows on a log-log scale calculated probability density functions (PDFs) $P(E)$ as functions of the sound energy E of the registered single acoustic events, for the fine (left panel) and coarse (right panel) toasted rusk rolls, each for different sample humidities. For each humidity, three different samples were fractured using the scalpel. E can be assumed to be proportional to the size of a fracture event [12,23]. The PDF is estimated as $P(E) \approx \frac{N_{E,E+\Delta E}}{\Delta E N_{tot}}$ with $N_{E,E+\Delta E}$ the number of observed events with energy between E and $E+\Delta E$ and N_{tot} the total number of observed events.

It is seen that the PDFs follow power laws over a range of about four orders of magnitude. These ranges are fitted to the

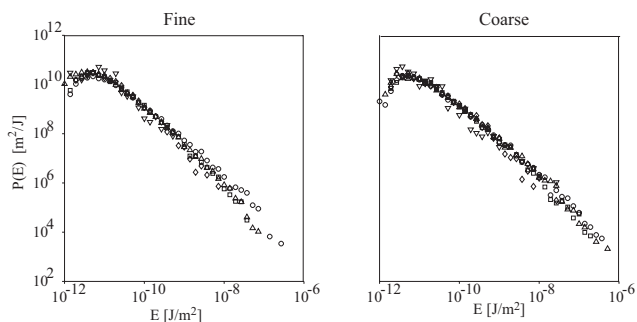


FIG. 5. PDF $P(E)$ of acoustic emissions as a function of their energy E during fracture of toasted rusk rolls having fine (left) and coarse (right) structures. RH=30% (○), 40% (△), 50% (□), 60% (◇), and 70% (△).

scaling law. Results of the fits for the two different morphologies and five different humidities are shown in Fig. 6. The characteristic exponents b are all around 1.5, as found for various crackling systems. However, small but clear differences between the scaling exponents b can be observed, indicating that the crackling phenomenon is not universal but dependent on the details of the system. For A_w smaller than 0.7, b increases when the cell wall material gets more viscous and the fracture becomes more viscoelastic, for both the fine and coarse structures. This supports the observations in earthquakes and rock fracture that b seems to be inversely proportional to the stress intensity factor [24,25], which decreases when the material becomes more viscous and less energy is available for crack extension. This is also in line with calculations performed by Olami *et al.* on a self-critical model to simulate earthquakes. They showed that b is negatively correlated with the level of conservation, i.e., the amount of force that is conserved during failure [26,27]. We also observed a larger b for the fine structure than for the coarse one. Clear differences between both structures in cell wall or beam thickness, and mechanical properties, are observed. The porosity of both structures is equal ($\phi \sim 0.9$) while the mean cell size of the coarse structure is about 0.23 mm and that of the fine structure 0.18 mm. This implies that the cell wall or beam thickness for the coarse structure is only about 1.2 times greater than that of the fine one. It has been suggested that a more localized failure would result in a higher b [14]. Although this is in line with the observed differences in cell wall or beam thickness and b , it is not likely that to be the explanation. More likely to explain a lower b for the coarse structure is the observation that the

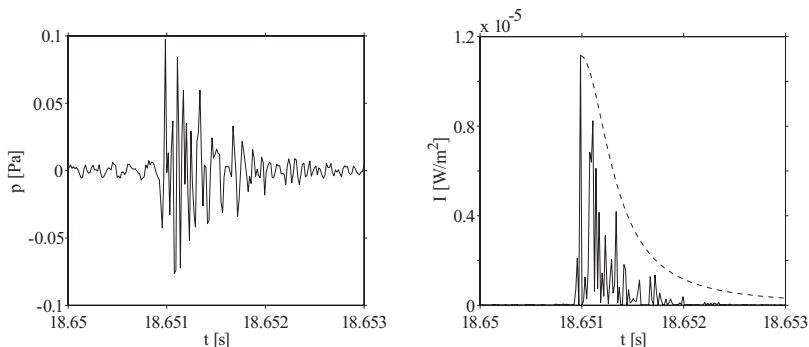


FIG. 4. Example of sound pressure (left) and intensity (right) of a single sound event (blowup of Fig. 2). The dashed line in the right graph corresponds to the envelope I_e (for explanation see text).

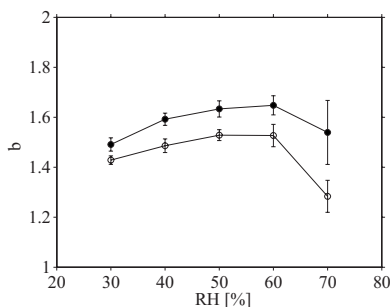


FIG. 6. Characteristic exponent b for fracture of toasted rusk rolls having fine (●) and coarse (○) structures for different relative humidities. Exponents and indicated errors are estimated from the PDFs shown in Fig. 6 using a least-squares fit of a linear function

coarse structure produces more sound than the fine structure upon failure, although the force needed is about equal. This is in line with the fact that consumers judge the coarse structure more crispy [22] than the fine one, and it indicates that the coarse structure fractures in a more brittle way and has a higher stress intensity factor, resulting in a lower b . However, further study is needed to be more quantitative. The same holds for the observed decrease of b at a RH value of 70%, which might be due to the fact that the system has gone through a glass transition, which occurs for these food systems and temperature at a RH of about 70% [28].

Similar power law behavior and dependence of b on humidity are observed when whole rusk rolls are fractured between plates covered with foam, although the absolute values seems to be somewhat smaller (about 0.1). Also other probes and deformation speeds were used. Typical examples for toasted rusk rolls equilibrated at 30% relative humidity are shown in Fig. 7. It indicates that the power law behavior of the fracture of toasted rusk rolls is, at least to a great extent, universal and independent of the method of fracturing. However, although b is for all experiments around 1.5, the value

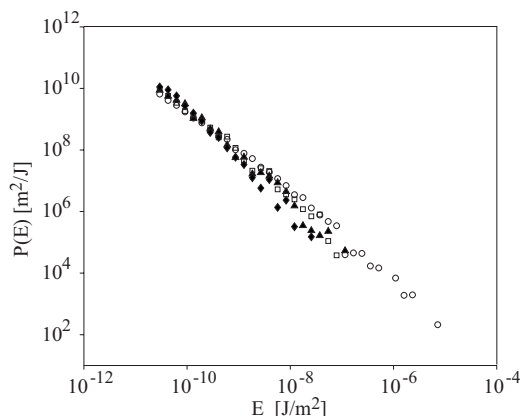


FIG. 7. PDF $P(E)$ of acoustic emissions as a function of their energy E during fracture of toasted rusk rolls (fine, RH=30%). (i) Whole rusk roll crushed between plates covered with foam at $v = 0.2$ mm/s (○, $b=1.4$), (ii) needle at $v=0.4$ mm/s (▲, $b=1.5$), (iii) scalpel at $v=0.4$ mm/s (□, $b=1.5$), and (iv) scalpel at $v = 0.1$ mm/s (◆, $b=1.7$).

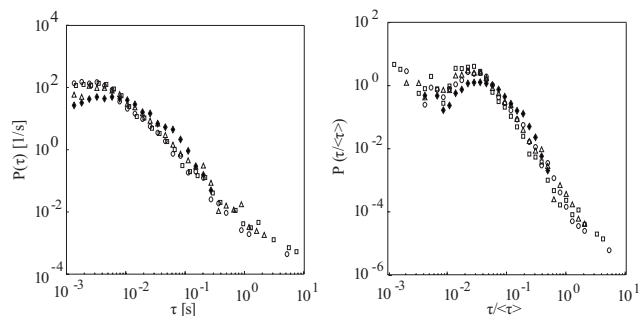


FIG. 8. PDF of delay times τ (left) and $\tau/\langle\tau\rangle$ (right) between successive acoustic emissions. Toasted rusk rolls are fractured using a scalpel (◆, fine, RH=30%) and crushed between two foam-covered plates (□, fine, RH=30%; ○, fine, RH=40%; △, coarse, RH=30%).

varies between $b=1.4$ and 1.6, indicating nonuniversality and dependence on the details of the system and even speed and method of deformation. It is interesting to note that the b value for low deformation speeds seems to be larger than for high deformation speeds. This may be due to some viscoelastic behavior of these systems that causes less energy to be available for crack formation and propagation at low deformation speed compared to high deformation speeds. This is in line with the observation that b is negatively correlated with the stress intensity factor.

We also studied the delay or waiting time τ between successive sound events. The duration of small audible sound pulses with sound pressure below approximately 0.01 Pa is about 1 ms, while that of larger pulses with sound pressures of a few pascals can be ten times larger. Furthermore, due to the signal to noise ratio of our experimental setup, we were not able to decrease the deformation speeds to such an extent that large waiting times of more than about 20 s could be measured. Therefore, only a range of τ of about three orders of magnitude could be measured. Figure 8 shows typical examples of the PDFs of waiting times $P(\tau)$ (left panel) and scaled waiting times $P(\tau/\langle\tau\rangle)$ (right panel) for different experiments. Here $\langle\tau\rangle$ is the average waiting time. For the fracture experiments using a scalpel, we did not find a clear power law behavior in the measurable range. For the failure experiments where the whole rusk roll was crushed between plates, power law behavior $P(\tau) \propto \tau^{-a}$ with a about 1.9 ± 0.2 was found. No clear correlation could be observed between the exponent a and the humidity, morphology, or method of fracture. This may be due to the large variation in a that was observed for the experiments performed under the same conditions. The observation that the recurrence time does not follows Omori's power law with a about unity [29] is most likely due to the fact that only long waiting times are measured. For this long time limit ($\tau \geq \langle\tau\rangle$), similar values of exponents a are found for the waiting times between earthquakes, rescaled according to the procedure proposed by Bak *et al.* [30,31], and crack propagation during fracture of Plexiglas [17].

IV. CONCLUSION

To conclude, we performed a detailed study of the fracture behavior of cellular food solids. Toasted rusk rolls hav-

ing different morphology and water content were fractured and the properties of single acoustic and force events determined. The intensities of the emitted sound events during fracture show power law behavior with critical exponents b of about 1.5, similar to what is found for other crackling phenomena. However, small differences in b for different sample humidity, sample morphology, and method of fracture were observed that could to a great extent be related to the amount of brittleness. Furthermore, power law scaling behavior is also observed for the waiting time distribution, with a characteristic exponent a about 1.9. This is near the characteristic exponents that have been found for distribu-

tions for long waiting times between earthquakes. These findings might help to elucidate the fracture behavior of cellular solids and give insights into the universality of the scaling behavior of fracture size and waiting times and how it depend on microscopic details of the system like viscoelasticity and morphology.

ACKNOWLEDGMENT

We acknowledge Eva M. Castro Prada for allowing us to use some of her fracture data.

-
- [1] S. P. Gross, J. Fineberg, M. Marder, W. D. McCormick, and H. L. Swinney, *Phys. Rev. Lett.* **71**, 3162 (1993).
- [2] M. Marder and X. Liu, *Phys. Rev. Lett.* **71**, 2417 (1993).
- [3] J. Boudet, S. Ciliberto, and V. Steinberg, *J. Phys. II* **6**, 1493 (1996).
- [4] J. Fineberg and M. Marder, *Phys. Rep.* **313**, 1 (1999).
- [5] T. Martín, P. Español, M. A. Rubio, and I. Zúñiga, *Phys. Rev. E* **61**, 6120 (2000).
- [6] M. Buehler and H. Gao, *Nature (London)* **439**, 307 (2006).
- [7] J. Sethna, K. Dahmen, and C. Myers, *Nature (London)* **410**, 242 (2001).
- [8] P. Bak, C. Tang, and K. Wiesenfeld, *Phys. Rev. Lett.* **59**, 381 (1987).
- [9] P. Bak, C. Tang, and K. Wiesenfeld, *Phys. Rev. A* **38**, 364 (1988).
- [10] C. Maes, A. Van Moffaert, H. Frederix, and H. Strauven, *Phys. Rev. B* **57**, 4987 (1998).
- [11] P. A. Houle and J. P. Sethna, *Phys. Rev. E* **54**, 278 (1996).
- [12] A. Petri, G. Paparo, A. Vespignani, A. Alippi, and M. Costantini, *Phys. Rev. Lett.* **73**, 3423 (1994).
- [13] L. I. Salminen, A. I. Tolvanen, and M. J. Alava, *Phys. Rev. Lett.* **89**, 185503 (2002).
- [14] L. Salminen, J. Pulakka, J. Rosti, M. Alava, and K. Niskanen, *Europhys. Lett.* **73**, 55 (2006).
- [15] A. Garcimartin, A. Guarino, L. Bellon, and S. Ciliberto, *Phys. Rev. Lett.* **79**, 3202 (1997).
- [16] A. Guarino, A. Garcimartin, and S. Ciliberto, *Eur. Phys. J. B* **6**, 13 (1998).
- [17] K. J. Maloy, S. Santucci, J. Schmittbuhl, and R. Toussaint, *Phys. Rev. Lett.* **96**, 045501 (2006).
- [18] J. Davidsen, S. Stanchits, and G. Dresen, *Phys. Rev. Lett.* **98**, 125502 (2007).
- [19] D. Stokes and A. Donald, *J. Mater. Sci.* **35**, 599 (2000).
- [20] A. Szczesniak, *Food Technol.* **44**, 86 (1990).
- [21] H. Luyten and T. van Vliet, *J. Texture Stud.* **37**, 221 (2006).
- [22] C. Primo-Martin, E. M. Castro-Prada, M. B. J. Meinders, P. F. G. Vereijken, and T. van Vliet, *Food Res. Int.* (in press), doi: 10.1016/j.foodres.2008.02.004.
- [23] M. Minozzi, G. Caldarelli, L. Pietronero, and S. Zapperi, *Eur. Phys. J. B* **36**, 203 (2003).
- [24] I. Main and P. Meredith, *Tectonophysics* **167**, 273 (1989).
- [25] D. Lockner, J. Byerlee, V. Kuksenko, A. Ponomarev, and A. Sidorin, *Nature (London)* **350**, 39 (1991).
- [26] Z. Olami, Hans Jacob S. Feder, and K. Christensen, *Phys. Rev. Lett.* **68**, 1244 (1992).
- [27] K. Christensen and Z. Olami, *Phys. Rev. A* **46**, 1829 (1992).
- [28] N. van Nieuwenhuijzen, R. Tromp, J. Mitchell, C. Primo-Martin, R. Hamer, and T. van Vliet (unpublished).
- [29] A. Saichev and D. Sornette, *Phys. Rev. Lett.* **97**, 078501 (2006).
- [30] P. Bak, K. Christensen, L. Danon, and T. Scanlon, *Phys. Rev. Lett.* **88**, 178501 (2002).
- [31] A. Corral, *Phys. Rev. Lett.* **92**, 108501 (2004).